Progress In Electromagnetics Research M, Vol. 72, 187–195, 2018

W-LS-IR Algorithm for Hybrid Precoding in Wideband Millimeter Wave MIMO Systems

Fulai Liu[1, 2, *], Ruiyan Du[1, 2], Xiaodong Kan[1, 2], and Xinwei Wang[1, 2]

Abstract—Hybrid analog/digital precoding is a promising technology that reduces the hardware complexity and power consumption of large-scale millimeter wave (mmWave) multiple-input multiple-output (MIMO) communication systems. Most prior work has focused on hybrid precoding for narrowband mmWave systems. MmWave systems, however, will likely act on wideband channels with frequency selectivity. Therefore, this paper presents an effective OFDM-based hybrid precoding algorithm (named as W-LS-IR algorithm) for wideband mmWave systems. Firstly, the initial phases of the analog precoding matrix are randomly generated, and the digital precoding matrix is initialized via the least squares (LS) method. Then, the column of the analog precoding matrix is derived from the dominant left singular vector of a residual matrix, and the corresponding row of the digital precoding matrix is updated using the LS method. Through the iterations of the aforementioned stage, the hybrid precoding matrix will approach a stable solution finally. Compared with related works, the proposed algorithm can improve the spectral efficiency of wideband mmWave MIMO communication systems. Simulation results are presented to confirm the efficiency of the proposed algorithm.

1. INTRODUCTION

Large bandwidths in the millimeter wave (mmWave) carrier frequencies provide high data rates for fifth generation (5G) communication systems [1]. Multiple input multiple output (MIMO) system is one of the promising techniques for exploiting the spectral efficiency of wireless channels. Unfortunately, the increased hardware cost and power consumption make full digital baseband precoder which requires the same number of radio frequency (RF) chains as the number of antenna elements infeasible for large-scale mmWave MIMO arrays [2]. To overcome this shortcoming, hybrid precoding structures have been introduced [2, 3], which comprise fewer RF chains than antenna elements.

Recently, several algorithms have been presented for the hybrid precoder. Most prior work on hybrid precoding has focused on narrowband channels. In [4], a transformation of the signals is adopted in the RF domain to reduce the number of RF chains and the phase shifter is designed by extracting MIMO channel state information (CSI). Based on the convex programming, hybrid precoding algorithms are studied in [3] and [5]. In [6], the non-convex matrix decomposition problem has been transformed into a series of convex sub-problems based on an alternate optimization technique. The convex quadratic programming method is exploited to obtain the analog precoding matrix, and the least squares (LS) method is used to calculate the digital precoding matrix. Based on the realistic subarray structure with low complexity, a near-optimal iterative hybrid analog-digital precoding scheme is presented in [7], where the successive interference cancellation is exploited to obtain the analog precoding matrix.

MmWave systems will likely operate on frequency selective channels [8]. Therefore, it is significant to develop the precoding schemes for wideband mmWave systems. One of the major challenges of

Received 28 June 2018, Accepted 23 August 2018, Scheduled 4 September 2018

* Corresponding author: Fulai Liu (fulailiu@126.com).

[1] Engineer Optimization & Smart Antenna Institute, Northeastern University at Qinhuangdao, Qinhuangdao, China. [2] School of Computer Science and Engineering, Northeastern University, Shenyang, China.

wideband mmWave OFDM-MIMO hybrid precoding systems is that the frequency selective transmission and reception will be deteriorated by the frequency-flat analog network. Limited work has been performed for wideband mmWave systems. In [1], the optimal baseband precoder for a given RF codebook is obtained, and an efficient codebook is designed for OFDM-based mmWave hybrid precoding systems. Based on Gram-Schmidt orthogonalization, a wideband greedy hybrid precoding algorithm is proposed in [9], which considers frequency selective hybrid precoding with RF precoding vectors taken from a quantized codebook. To overcome the frequency selectivity, a frequency selective delay compensation is given for wideband channels [10]. Based on the well-known Arnoldi iteration and the block coordinate descent (BCD), the precoding optimization algorithms are proposed in [11] and [12], respectively. The works in [13] and [14] have studied the iterative column maximization algorithm and the iterative coordinate descent algorithm for sharing array precoding matrices. A multi-beam transmission diversity scheme based on the hybrid precoding structure is introduced in [15], which is a single-stream transmission of MIMO-OFDM systems. In order to extend the approaches originally constructed for narrowband systems to wideband, multicarrier transceiver is designed for a single-link mmWave transmission and several simplifications are made to solve the optimization problems [16]. To maximize the overall spectral efficiency of wideband systems with much fewer RF chains, the OFDM-based hybrid precoding design for large-scale mmWave MIMO system is presented in [17]. The works [16, 17] commonly demonstrate that OFDM-based mmWave MIMO systems can exploit more throughput gains to design the frequency-flat analog precoders and multiple frequency selective digital precoders to achieve accurate alignment with frequency selective channel subspaces.

In this paper, a new wideband hybrid precoding algorithm is developed for mmWave MIMO systems. The proposed algorithm assumes that an initial analog precoding matrix is randomly generated firstly. The corresponding digital precoding matrix is initialized by exploiting the LS method. Then, the largest left-singular vector of a residual matrix is solved by using the power method. Based on that, the hybrid precoding vectors are updated alternately. Therefore, through the iterations of the aforementioned stage, the hybrid precoding matrix will approach a stable solution finally, so that the proposed W-LS-IR algorithm can further improve the spectral efficiency.

The rest of the paper is organized as follows. Section 2 briefly introduces the adopted system and the channel model for OFDM-based wideband mmWave hybrid analog-digital precoding. The proposed W-LS-IR algorithm is developed in detail in Section 3. Section 4 presents several simulation results to verify the performance of the proposed algorithm. Finally, the concluding remark is provided in Section 5.

2. SYSTEM MODEL

Consider an OFDM-based wideband mmWave communication system with K subcarriers as shown in Figure 1. A base station (BS) with N_t antennas and N_{RF} RF chains is assumed to communicate with a single mobile station (MS) with N_r antennas and N_{RF} RF chains. The number of length-K data symbol blocks is denoted by N_s. In fact, the number of RF chains at the MS's is usually less than that of the BS's. For simplicity, we use an equal number of RF chains at the transmitter and receiver, such that $N_s \leq N_{RF} \leq \min(N_t, N_r)$.

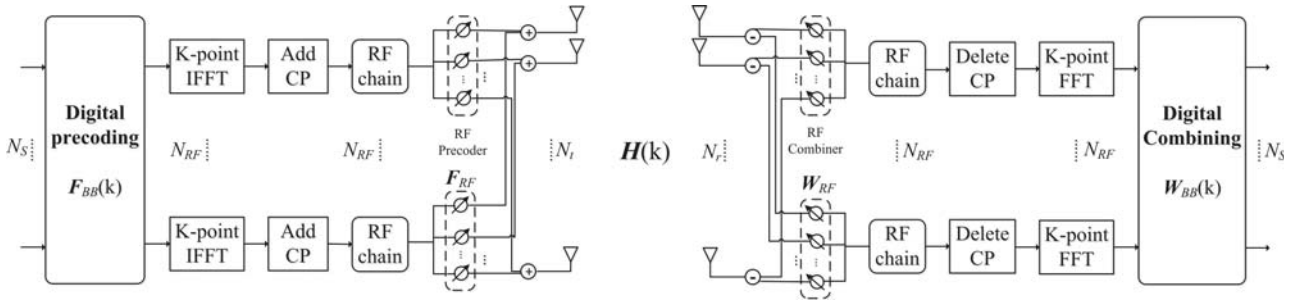

Figure 1. A block diagram of the OFDM based BS-MS transceiver that employs hybrid analog-digital precoding.

At the transmitter, the discrete-time transmitted signal at subcarrier k can be written as [11]

$$\mathbf{x}(k) = \mathbf{F}_{RF}\mathbf{F}_{BB}(k)\mathbf{s}(k), \quad k = 1, 2, \ldots, K \tag{1}$$

where $\mathbf{F}_{BB}(k) \in \mathbb{C}^{N_{RF} \times N_s}$ and $\mathbf{F}_{RF} \in \mathbb{C}^{N_t \times N_{RF}}$ stand for the digital baseband precoding matrix at subcarrier k and the analog RF precoding matrix respectively. Note that the model assumes that all subcarriers are used; therefore, the data block length is equal to the number of subcarriers. It is important to emphasize that the RF precoding matrix $\mathbf{F}_{RF}$ is the same for all subcarriers. This means that the RF precoder is assumed to be frequency flat while the baseband precoders can be different for each subcarrier. $\mathbf{s}(k) \in \mathbb{C}^{N_s \times 1}$ is the symbol vector such that $\mathbb{E}[\mathbf{s}(k)\mathbf{s}(k)^H] = \frac{1}{KN_S}\mathbf{I}_{N_S}$, where $\mathbf{I}_{N_S}$ is the identify matrix, and $\mathbb{E}[\cdot]$ stands for the expectation operator. Since the analog RF precoding matrix $\mathbf{F}_{RF}$ is implemented by using analog phase shifters, the entries of $\mathbf{F}_{RF}$ are subject to the constant modulus constraint. To reflect that, the constraint can be given by $|\mathbf{F}_{RF(m,n)}| = 1$. The normalized transmit power constraint is given by $\|\mathbf{F}_{RF}\mathbf{F}_{BB}(k)\|_F^2 = N_s$ in which $|\cdot|$ is the determinant, $\|\cdot\|_F$ denotes the Frobenius norm.

At the MS, assuming perfect carrier and frequency offset synchronization, the received signal at subcarrier k after processing can be expressed as [9]

$$\mathbf{y}(k) = \sqrt{\rho}\mathbf{W}_{BB}^H(k)\mathbf{W}_{RF}^H\mathbf{H}(k)\mathbf{F}_{RF}\mathbf{F}_{BB}(k)\mathbf{s}(k) + \mathbf{W}_{BB}^H(k)\mathbf{W}_{RF}^H\mathbf{n}(k) \tag{2}$$

where $\mathbf{H}(k)$ denotes the $N_r \times N_t$ channel matrix at subcarrier k, and ρ is the average received power. $\mathbf{W}_{RF} \in \mathbb{C}^{N_r \times N_{RF}}$ and $\mathbf{W}_{BB}(k) \in \mathbb{C}^{N_{RF} \times N_s}$ stand for the analog combining matrix and the digital combining matrix, respectively. $\mathbf{n}(k)$ is a Gaussian noise vector which follows the Gaussian distribution $\mathcal{CN}(0, \sigma_n^2)$, where σ_n^2 denotes the noise power. The superscript $(\cdot)^H$ stands for the Hermitian transpose.

The wideband channel matrix $\mathbf{H}(k)$ is composed of N_{cl} clusters, and each cluster consists of N_{ray} rays. Let $L = N_{cl}N_{ray}$ be the total number of propagation paths, and the channel matrix at subcarrier k can be expressed as

$$\mathbf{H}(k) = \sqrt{\frac{N_t N_r}{L}} \sum_{i=1}^{N_{cl}} \sum_{l=1}^{N_{ray}} \alpha_{il} e^{j2\pi\tau_{il}f_k} \mathbf{a}_r(\phi_{il}^r, \theta_{il}^r)\mathbf{a}_t(\phi_{il}^t, \theta_{il}^t)^H \tag{3}$$

where α_{il} is the complex path gain of lth ray in ith cluster; τ_{il} stands for the relative time delay from each cluster; f_k represents the center frequency of subcarrier k. The array response vectors of uniform planar array (UPA) $\mathbf{a}_r(\phi_{il}^r, \theta_{il}^r)$ and $\mathbf{a}_t(\phi_{il}^t, \theta_{il}^t)$ represent the receive and transmit array response vectors, where $\phi_{il}^r(\phi_{il}^t)$ and $\theta_{il}^r(\theta_{il}^t)$ stand for azimuth and elevation angles of arrival and departure (AoAs and AoDs), respectively.

The array response vector for an $M \times N$ UPA is defined as [18]

$$\begin{aligned}\mathbf{a}_{\mathrm{UPA}}(\phi_{il}, \theta_{il}) \;=\; & \frac{1}{\sqrt{MN}}\Big[1 \quad \ldots \quad e^{j\frac{2\pi}{\lambda}d(p\cos\phi_{il}\sin\theta_{il} + q\sin\phi_{il}\sin\theta_{il})} \\ & \ldots \quad e^{j\frac{2\pi}{\lambda}d((M-1)\cos\phi_{il}\sin\theta_{il} + (N-1)\sin\phi_{il}\sin\theta_{il})}\Big]^{\mathrm{T}}\end{aligned} \tag{4}$$

where $0 \le p \le M$ and $0 \le q \le N$ are the antenna elements on the 2D plane; d denotes the antenna spacing; λ is the signal wavelength; $[\cdot]^{\mathrm{T}}$ stands for the transpose.

Assume that the CSI is perfect. When Gaussian symbols are transmitted over the mmWave channel, the average achievable spectrum efficiency R can be obtained by [3]

$$\begin{aligned}R \;=\; & \frac{1}{K}\sum_{k=1}^{K} \log_2\Big(\Big|\mathbf{I}_{N_s} + \frac{\rho}{N_s}\mathbf{R}_n^{-1}(k)\mathbf{W}_{BB}^H(k)\mathbf{W}_{RF}^H\mathbf{H}(k)\mathbf{F}_{RF}\mathbf{F}_{BB}(k) \\ & \times\mathbf{F}_{BB}^H(k)\mathbf{F}_{RF}^H\mathbf{H}^H(k)\mathbf{W}_{RF}\mathbf{W}_{BB}(k)\Big|\Big)\end{aligned} \tag{5}$$

where $\mathbf{R}_n(k) = \sigma_n^2\mathbf{W}_{BB}^H(k)\mathbf{W}_{RF}^H\mathbf{W}_{RF}\mathbf{W}_{BB}(k)$ is the noise covariance matrix of the subcarrier k after being processed by the receiver.

From Eq. (5), it is clear that directly maximizing the spectral efficiency R requires a joint optimization over $(\mathbf{F}_{RF}, \mathbf{F}_{BB}(k), \mathbf{W}_{RF}, \mathbf{W}_{BB}(k))$, which is intractable. Fortunately, the joint design

problem can be separated into two sub-problems, namely, the precoding and combining sub-problems, which have similar mathematical formulations. The aim of this paper, which will mainly focus on the precoder design, is to develop a new hybrid precoding design to maximize the achievable system spectral efficiency. The proposed algorithm can be applied to the combiner equivalently.

The precoder optimization problem can be expressed as [10]

$$\begin{aligned} \underset{\mathbf{F}_{RF},\mathbf{F}_{BB}(k)}{\text{minimize}} & \sum_{k=1}^{K} \|\mathbf{F}_{\text{opt}}(k) - \mathbf{F}_{RF}\mathbf{F}_{BB}\,(k)\,\|_F^2 \\ \text{s.t.} & \,|\mathbf{F}_{RF(m,n)}| = 1 \\ & \sum_{k=1}^{K} \|\mathbf{F}_{RF}\mathbf{F}_{BB}(k)\|_F^2 = KN_s \end{aligned} \tag{6}$$

where the $N_t \times N_s$ matrix $\mathbf{F}_{\text{opt}}(k) = \mathbf{V}(k)_{:,1;N_s}$ is the optimal full digital precoding matrix given by the singular value decomposition (SVD) of wideband channel matrix $\mathbf{H}(k)$ at subcarrier k, i.e., $\mathbf{H}(k) = \mathbf{U}(k)\mathbf{\Sigma}(k)\mathbf{V}(k)^H$.

Since Eq. (6) contains multiple subcarriers which share the analog precoding matrix and there is coupling between the baseband and RF precoders, which arises in the power constraint, it is difficult to find the optimal solution. Therefore, the optimization problem in Eq. (6) can be transformed into the matrix connection problem [19] and reformulated as

$$\begin{aligned} \underset{\mathbf{F}_{RF},\tilde{\mathbf{F}}_{BB}}{\text{minimize}} & \|\tilde{\mathbf{F}}_{\text{opt}} - \mathbf{F}_{RF}\tilde{\mathbf{F}}_{BB}\|_F^2 \\ \text{s.t.} & \,|\mathbf{F}_{RF(m,n)}| = 1 \\ & \|\mathbf{F}_{RF}\tilde{\mathbf{F}}_{BB}\|_F^2 = KN_s \end{aligned} \tag{7}$$

where $\tilde{\mathbf{F}}_{\text{opt}} = [\mathbf{F}_{\text{opt}}(1), \mathbf{F}_{\text{opt}}(2), \ldots, \mathbf{F}_{\text{opt}}(K)]$, $\tilde{\mathbf{F}}_{BB} = [\mathbf{F}_{BB}(1), \mathbf{F}_{BB}(2), \ldots, \mathbf{F}_{BB}(K)]$.

Unfortunately, it is still intractable to solve the optimization problem in Eq. (7) due to the constant modulus constraint of the analog precoder $\mathbf{F}_{RF}$. To solve this issue, the problem in Eq. (7) will be analyzed from successive iterative refinement in detail in the following sections.

3. ALGORITHM FORMULATION

In this section, an effective hybrid precoding algorithm (named as W-LS-IR algorithm) is proposed for wideband mmWave communication systems. The specific process will be described in the rest of this section.

3.1. Analog Precoding Matrix Refinement

In order to develop an efficient iterative refinement algorithm and improve the performance of the hybrid precoder further, the initial phases of the analog RF precoding matrix $\mathbf{F}_{RF}$ can be generated randomly, and the corresponding digital precoding matrix $\tilde{\mathbf{F}}_{BB}$ is initialized by using the LS method, so that the hybrid precoder progressively approaches the optimal full digital precoder. The residual μ can be defined as

$$\mu = \|\tilde{\mathbf{F}}_{\text{opt}} - \mathbf{F}_{RF}\tilde{\mathbf{F}}_{BB}\|_F^2 = \left\| \tilde{\mathbf{F}}_{\text{opt}} - \sum_{i=1}^{N_{RF}} \mathbf{f}_{RF,i}\tilde{\mathbf{f}}_{BB,i}^H \right\|_F^2 \tag{8}$$

where $\mathbf{f}_{RF,i} \in \mathbb{C}^{N_t \times 1}$ denotes the ith column of the analog RF precoder $\mathbf{F}_{RF}$, and $\tilde{\mathbf{f}}_{BB,i}^H \in \mathbb{C}^{1 \times N_s}$ is the ith row of the digital precoder $\tilde{\mathbf{F}}_{BB}$. In each refinement process, only one column of the analog RF precoder $\mathbf{F}_{RF}$ and one corresponding row of the digital precoder $\tilde{\mathbf{F}}_{BB}$ are updated, and other columns

of $\mathbf{F}_{RF}$ and rows of $\tilde{\mathbf{F}}_{BB}$ are fixed. Then, the minimization problem of the residual μ given by Eq. (8) can be reformulated as

$$\arg\min_{\mathbf{f}_{RF,j},\tilde{\mathbf{f}}_{BB,j}^H} \left\| \tilde{\mathbf{F}}_{\text{opt}} - \sum_{i\neq j}^{N_{RF}} \mathbf{f}_{RF,i}\tilde{\mathbf{f}}_{BB,i}^H - \mathbf{f}_{RF,j}\tilde{\mathbf{f}}_{BB,j}^H \right\|_F^2 = \left\| \tilde{\mathbf{E}}_j - \mathbf{f}_{RF,j}\tilde{\mathbf{f}}_{BB,j}^H \right\|_F^2 \tag{9}$$

where $\mathbf{f}_{RF,j}$ is the column of the analog RF precoder $\mathbf{F}_{RF}$ that needs to be refined and the corresponding row of the digital precoder $\tilde{\mathbf{F}}_{BB}$ denoted by $\tilde{\mathbf{f}}_{BB,j}^H$. $\tilde{\mathbf{E}}_j$ stands for the residual matrix.

Assume that the unit-modulus constraint is not considered. According to the Eckart-Young-Mirsky theorem [20], the problem in Eq. (9) can be rewritten as

$$\arg\min_{\mathbf{f}_{RF,j}} \|\tilde{\mathbf{E}}_j - \sigma_1 \mathbf{u}_1 \mathbf{v}_1^H\|_F^2 \tag{10}$$

where σ_1 is the largest singular value of residual matrix $\tilde{\mathbf{E}}_j$, and $\mathbf{u}_1$ and $\mathbf{v}_1$ are the first left and first right singular vectors of $\tilde{\mathbf{E}}_j$, respectively, i.e., $\mathbf{f}_{RF,j} = \mathbf{u}_1$.

Considering the unit-modulus constraint, it is easy to know the global optimal solution of the problem in Eq. (10) by

$$\mathbf{f}_{RF,j} = e^{j\angle \mathbf{u}_1} \tag{11}$$

where $\angle \mathbf{u}_1$ denotes the phase vector of $\mathbf{u}_1$, which means that the element of $\mathbf{f}_{RF,j}$ will share the same phase as the corresponding element of $\mathbf{u}_1$ with amplitude of one.

3.2. Digital Precoding Matrix Refinement

With the fixed column of the analog RF precoder $\mathbf{f}_{RF,j}$, the problem in Eq. (9) can be expressed as

$$\arg\min_{\tilde{\mathbf{f}}_{BB,j}^H} \|\tilde{\mathbf{E}}_j - \mathbf{f}_{RF,j}\tilde{\mathbf{f}}_{BB,j}^H\|_F^2 \tag{12}$$

The global optimal solution of the problem in Eq. (12) can be given by the well-known LS method. Therefore

$$\tilde{\mathbf{f}}_{BB,j}^H = \mathbf{f}_{RF,j}^{\dagger}\tilde{\mathbf{E}}_j = \frac{1}{N_t}\mathbf{f}_{RF,j}^H\tilde{\mathbf{E}}_j \tag{13}$$

where $(\cdot)^{\dagger}$ stands for the pseudo-inverse. Repeat Eqs. (11) and (13) until all the columns of $\mathbf{F}_{RF}$ and all the rows of $\tilde{\mathbf{F}}_{BB}$ are considered.

Based on the above discussion, it is clear that the proposed hybrid precoding algorithm for wideband mmWave systems can be summarized and presented with pseudo-codes in Table 1.

As shown in Table 1, the proposed W-LS-IR algorithm sets the initial analog RF precoding matrix $\mathbf{F}_{RF}$ randomly, and the corresponding digital precoding matrix is obtained from $\tilde{\mathbf{F}}_{BB} = \mathbf{F}_{RF}^{\dagger}\tilde{\mathbf{F}}_{\text{opt}}$. Moreover, the refining stages of analog precoder (step 2 to step 3) are executed to update the vector $\mathbf{f}_{RF,i}$. It is easy to see that step 4 is used to update the vector $\tilde{\mathbf{f}}_{BB,i}^H$. Besides, step 6 calculates the residual μ between the matrix $\tilde{\mathbf{F}}_{\text{opt}}$ and the product of $\mathbf{F}_{RF}\tilde{\mathbf{F}}_{BB}$. The residual is stored for the comparison later. Step 3 and step 7 are used to satisfy the unit-modulus constraint and the transmitter power constraint, respectively. Then, the updated matrices $\mathbf{F}_{RF}$ and $\tilde{\mathbf{F}}_{BB}$ are used as a new input to the step 1 to step 4 for the next iteration. The process continues until $|\mu^{t-1} - \mu^t| \leq \varepsilon$, where ε denotes the threshold.

3.3. Computational Complexity Analysis

In this subsection, we briefly investigate the computational complexity of the proposed W-LS-IR algorithm. For the OFDM-based wideband mmWave MIMO systems shown in Figure 1, Table 2 presents the computational complexity of the W-LS-IR algorithm detailedly. Specially, the computational complexity mainly includes:

Table 1. W-LS-IR algorithm

Input: $\tilde{\mathbf{F}}_{\text{opt}}$, N_{RF}, N_s, N_t, ε

Initializations:

$\mathbf{F}_{RF}$ is given randomly, $\tilde{\mathbf{F}}_{BB} = \mathbf{F}_{RF}^{\dagger}\tilde{\mathbf{F}}_{\text{opt}}$, $t = 0$

repeat

for $j = 1 \rightarrow N_{RF}$ **do**

1: $\tilde{\mathbf{E}}_j = \tilde{\mathbf{F}}_{\text{opt}} - \sum_{i \neq j}^{N_{RF}} \mathbf{f}_{RF,i}^{(t)} \tilde{\mathbf{f}}_{BB,i}^{(t)H}$

2: Compute $\mathbf{u}_1$ of $\tilde{\mathbf{E}}_j$ by the power method

3: $\mathbf{f}_{RF,i} = e^{j\angle \mathbf{u}_1}$

4: $\tilde{\mathbf{f}}_{BB,i}^{H} = \frac{1}{N_t}\mathbf{f}_{RF,i}^{H}\tilde{\mathbf{F}}_{\text{opt}}$

end for

5: $t = t + 1$

6: $\mu^t = \|\tilde{\mathbf{F}}_{\text{opt}} - \mathbf{F}_{RF}\tilde{\mathbf{F}}_{BB}\|_F^2$

until $|\mu^{t-1} - \mu^t| \leq \varepsilon$

7: $\tilde{\mathbf{F}}_{BB} = \sqrt{KN_s}\frac{\tilde{\mathbf{F}}_{BB}}{\|\mathbf{F}_{RF}\tilde{\mathbf{F}}_{BB}\|_F}$

Output: $\mathbf{F}_{RF}$, $\tilde{\mathbf{F}}_{BB}$.

Table 2. Complexity of the W-LS-IR algorithm.

Operation	Complexity
$\tilde{\mathbf{E}}_j = \tilde{\mathbf{F}}_{\text{opt}} - \sum_{i \neq j}^{N_{RF}} \mathbf{f}_{RF,i}^{(t)} \tilde{\mathbf{f}}_{BB,i}^{(t)H}$	$\mathcal{O}(Kk_1N_tN_sN_{RF}(N_{RF}-1))$
$\mathbf{f}_{RF,i} = e^{j\angle \mathbf{u}_1}$	$\mathcal{O}(Kk_1k_2N_tN_sN_{RF})$
$\tilde{\mathbf{f}}_{BB,i}^{H} = \frac{1}{N_t}\mathbf{f}_{RF,i}^{H}\tilde{\mathbf{F}}_{\text{opt}}$	$\mathcal{O}(Kk_1N_tN_sN_{RF})$
$\mu^t = \|\tilde{\mathbf{F}}_{\text{opt}} - \mathbf{F}_{RF}\tilde{\mathbf{F}}_{BB}\|_F^2$	$\mathcal{O}(Kk_1N_tN_s)$
$\mathbf{F}_{BB} = \sqrt{N_s}\frac{\mathbf{F}_{BB}}{\|\mathbf{F}_{RF}\mathbf{F}_{BB}\|_F}$	$\mathcal{O}(k_1N_tN_{RF}N_s)$

- The computational complexity of the residual matrix $\tilde{\mathbf{E}}_j$ in step 1, of the order $\mathcal{O}(Kk_1N_tN_sN_{RF}(N_{RF}-1))$, where k_1 is the number of iterations of the proposed algorithm.
- The computational complexity of the refined jth column of the analog RF precoder $\mathbf{F}_{RF}$ by using the power method and the refined jth row of the digital precoder $\tilde{\mathbf{F}}_{BB}$ by exploiting the LS method in step 2 to step 4, i.e., $\mathbf{f}_{RF,i}$ and $\tilde{\mathbf{f}}_{BB,i}^{H}$, of the orders $\mathcal{O}(Kk_1k_2N_tN_sN_{RF})$ and $\mathcal{O}(Kk_1N_tN_sN_{RF})$, respectively, where k_2 is the number of iterations of power method.
- The computational complexity of the residual value μ in step 6, of the order $\mathcal{O}(Kk_1N_tN_s)$.

With respect to the iterative procedure, the complexity of the proposed W-LS-IR algorithm is similar to the OMP-based sparse hybrid precoding algorithm in [2] and the PE-AltMin algorithm in [3]. However, the simulation results in the next section can prove that the proposed algorithm has better spectral efficiency than the algorithms in [2] and [3].

4. SIMULATION RESULTS

In this section, we construct several simulations to evaluate the performance of the proposed W-LS-IR algorithm for OFDM-based single-user wideband mmWave MIMO communication systems as shown in Figure 1. For all terminals, equipped with UPA on the 2D plane, the number of wideband subcarriers is $K = 128$. The BS and MS are composed of 12×12 and 6×6 antenna elements, respectively. The

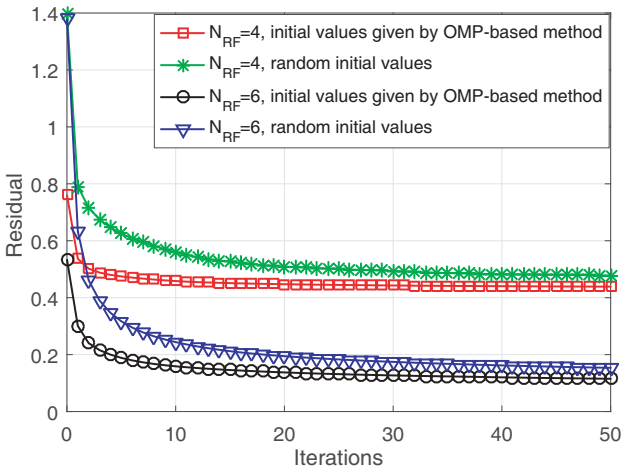

Figure 2. Residual for various iterations.

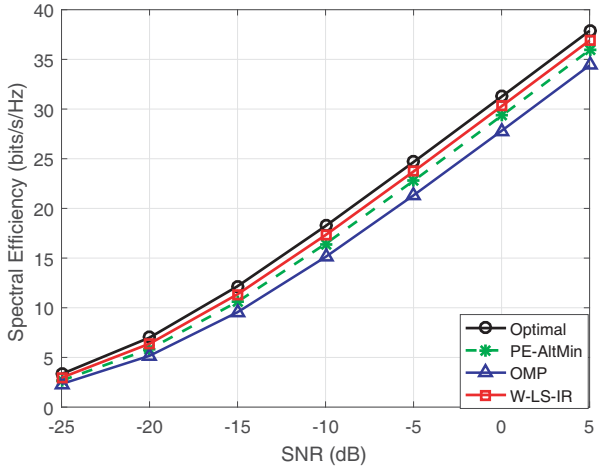

Figure 3. Spectral efficiency for various SNR.

mmWave propagation channel is modeled as $L = N_{cl}N_{ray} = 50$ paths, which are divided into $N_{cl} = 5$ and $N_{ray} = 10$. When the signal leaves the transmitter, the average azimuth/elevation AoD of each cluster, i.e., $\phi^t_{\mathcal{C}_i} = \frac{1}{10}\sum_{l\in\mathcal{C}_i}\phi^t_l$, $\theta^t_{\mathcal{C}_i} = \frac{1}{10}\sum_{l\in\mathcal{C}_i}\theta^t_l$ $(i = 1, 2, \ldots, 5)$, follow uniform distribution within $0 < \phi^t_{\mathcal{C}_i} < 2\pi$, $0 < \theta^t_{\mathcal{C}_i} < 2\pi$, i.e., $\phi^t_{\mathcal{C}_i} \sim \mathcal{U}(0, 2\pi)$, $\theta^t_{\mathcal{C}_i} \sim \mathcal{U}(0, 2\pi)$. The azimuth/elevation AoD of rays in each cluster obeys Laplace distribution, i.e., $\phi^t_{l,l\in\mathcal{C}_i} \sim \mathcal{L}(\mu^t_{\phi,\mathcal{C}_i}, b^t_{\phi,\mathcal{C}_i})$, $\theta^t_{l,l\in\mathcal{C}_i} \sim \mathcal{L}(\mu^t_{\theta,\mathcal{C}_i}, b^t_{\theta,\mathcal{C}_i})$, where $\mu^t_{\phi,\mathcal{C}_i} = \phi^t_{\mathcal{C}_i}$, $\mu^t_{\theta,\mathcal{C}_i} = \theta^t_{\mathcal{C}_i}$ are the location parameters, and $b^t_{\phi,\mathcal{C}_i} = b^t_{\theta,\mathcal{C}_i} = 10^\circ$ are the scale parameters. The statistic properties of azimuth/elevation AoA are the same as the azimuth/elevation AoD. The distance between the antennas is a half wavelength. The threshold is set as $\varepsilon = 0.1$. It is assumed that the perfect CSI is known at both BS and MS instantaneously. All the results are the average of 1000 channel realizations.

Figure 2 shows the residuals of the hybrid precoder given by the proposed W-LS-IR algorithm when $N_s = 4$. As can be seen from Figure 2, compared with random initial values, the initial values given by the OMP-based sparse method in [2] have a fairly high convergence rate to reach a stable point. Also, it is easy to see that different initial values give similar stable points eventually. In other words, the stable point of the proposed algorithm is insensitive to the initial values. So, the following simulations of the proposed algorithm are obtained with random initial values.

Figure 3 plots the spectral efficiencies achieved with the optimal full digital precoder, the OMP-based sparse precoding algorithm in [2], the PE-AltMin algorithm in [3] and the proposed W-LS-IR algorithm when $N_s = 4$ and $N_{RF} = 5$. It can be observed that with the increase of SNR, the performances of all algorithms gradually improve, while the proposed W-LS-IR algorithm outperforms them. Moreover, the proposed algorithm performs close to the optimal precoder. This means that the proposed W-LS-IR algorithm can improve the spectral efficiency effectively.

Figure 4 shows the spectral efficiencies given by different hybrid precoding algorithms and the optimal full digital algorithm with various N_{RF} when SNR $= -5$ dB and $N_s = 4$. It can be observed that the proposed W-LS-IR algorithm outperforms the OMP-based sparse precoding algorithm in [2] and the PE-AltMin algorithm in [3] when $N_{RF}>N_S$. Also, with the growth of the number of N_{RF}, the spectral efficiency gap between the proposed algorithm and the optimal full digital precoder decreases gradually, and when $N_{RF} = 8$, this gap is less than 0.1 bit/s/Hz. Hence, the improvements given by the proposed W-LS-IR algorithm are consistent in most of the cases.

Figure 5 shows the spectral efficiencies achieved by the different algorithms with the number of paths L. Assume that each cluster has the same number of paths with $N_{cl} = 5$, SNR $= 5$ dB, $N_s = 4$ and $N_{RF} = 5$. It is observed that the proposed algorithm always outperforms the OMP-based algorithm in [2] and the PE-AltMin algorithm in [3]. Additionally, the spectral efficiency gap between the proposed algorithm and the optimal full digital precoder becomes higher with the growth of propagation paths. Therefore, the proposed W-LS-IR algorithm is more applicable to sparse channels than rich channels.

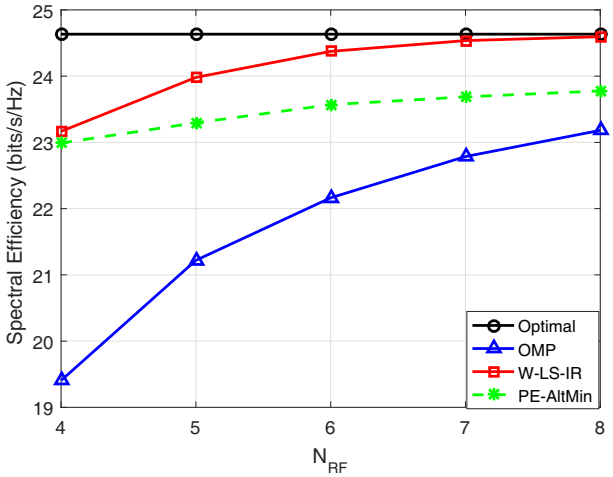

Figure 4. Spectral efficiency for various N_{RF}.

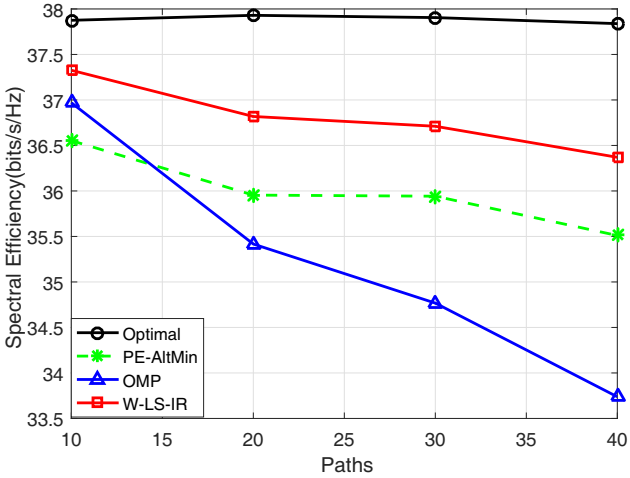

Figure 5. Spectral efficiency for various paths.

5. CONCLUSION

In this paper, a hybrid precoding algorithm is considered for wideband mmWave MIMO systems. The analog precoding vectors are updated by the power method, and then the digital precoding vectors are compensated by the LS method. The two phases are implemented alternatively, and the residual decreases gradually until the iteration termination condition is satisfied. Simulation results show that the presented algorithm can not only be exploited for wideband mmWave systems but also improve the spectral efficiency effectively of mmWave MIMO communication systems. Specially, future work related to such mmWave precoding includes relaxing the assumptions made throughout this paper such as (i) perfect CSI at both BS and MS, (ii) knowledge of the antenna array structure, and (iii) perfect carrier and frequency offset synchronization.

ACKNOWLEDGMENT

This work was supported by the Natural Science Foundation of Hebei Province (No. F2016501139) and the Fundamental Research Funds for the Central Universities under Grant No. N162304002 and No. N172302002, and the National Natural Science Foundation of China under Grant No. 61501102 and No. 61473066.

REFERENCES

1. Alkhateeb, A. and R. W. Heath, "Frequency selective hybrid precoding for limited feedback millimeter wave systems," *IEEE Transactions on Communications*, Vol. 64, No. 5, 1801–1818, 2015.
2. Ayach, O. E., S. Rajagopal, S. Abu-Surra, Z. Pi, and R. W. Heath, Jr., "Spatially sparse precoding in millimeter wave MIMO systems," *IEEE Transactions Wireless Communications*, Vol. 13, No. 3, 1499–1513, 2014.
3. Yu, X., J. C. Shen, J. Zhang, and K. B. Letaief, "Alternating minimization algorithms for hybrid precoding in millimeter wave MIMO systems," *IEEE Journal of Selected Topics in Signal Processing*, Vol. 10, No. 3, 485–500, 2016.
4. Zhang, A., F. Molisch, and S. Y. Kung., "Variable-phase-shift-based RF-baseband codesign for MIMO antenna selection," *IEEE Transactions on Signal Processing*, Vol. 53, No. 11, 4091–4103, 2005.

5. Rusu, C., R. Mendez-Rial, N. Gonzalez-Prelcic, and R. W. Heath, "Low complexity hybrid precoding strategies for millimeter wave communication systems," *IEEE Transactions on Wireless Communications*, Vol. 15, No. 12, 8380–8393, 2016.
6. Ni, W., X. Dong, and W. S. Lu., "Near-optimal hybrid processing for massive mimo systems via matrix decomposition," *IEEE Transactions on Signal Processing*, Vol. 65, No. 15, 3922–3933, 2017.
7. Dai, L., X. Gao, J. Quan, S. Han, and C. L. I, "Near-optimal hybrid analog and digital precoding for downlink mmWave massive MIMO systems," *IEEE International Conference on Communications*, 1334–1339, 2015.
8. Pi, Z. and F. Khan, "An introduction to millimeter-wave mobile broadband systems," *IEEE Communications Magazine*, Vol. 49, No. 6, 101–107, 2011.
9. Alkhateeb, A. and R. W. Heath, "Gram schmidt based greedy hybrid precoding for frequency selective millimeter wave MIMO systems," *IEEE International Conference on Acoustics, Speech and Signal Processing*, 3396–3400, 2016.
10. Wang, G., J. Sun, and G. Ascheid, "Hybrid beamforming with time delay compensation for millimeter wave mimo frequency selective channels," *IEEE Vehicular Technology Conference*, 1–6, 2016.
11. Ghauch, H., M. Bengtsson, T. Kim, and M. Skoglund, "Subspace estimation and decomposition for hybrid analog-digital millimetre-wave MIMO systems," *IEEE Vehicular Technology Conference*, 395–399, 2015.
12. Ghauch, H., T. Kim, M. Bengtsson, and M. Skoglind, "Subspace estimation and decomposition for large millimeter-wave MIMO systems," *IEEE Journal of Selected Topics in Signal Processing*, Vol. 10, No. 3, 528–542, 2015.
13. Foad, S. and Y. Wei, "Hybrid digital and analog beamforming design for large-scale antenna arrays," *IEEE Journal on Selected Topics in Signal Processing*, Vol. 10, No. 3, 501–513, 2016.
14. Foad, S. and Y. Wei, "Hybrid digital and analog beamforming design for large-scale MIMO systems," *IEEE International Conference on Acoustics, Speech and Signal Processing*, 2929–2933, 2015.
15. Kim, C., T. Kim, and J. Y. Seol, "Multi-beam transmission diversity with hybrid beamforming for MIMO-OFDM systems," *IEEE Globecom Workshops*, 61–65, 2013.
16. Iwanow, M., N. Vuci, M. H. Castaneda, J. Luo, W. Xu, and W. Utschick, "Some aspects on hybrid wideband transceiver design for mmWave communication systems," *ITG-Fachbericht-WSA*, 1–8, 2016.
17. Sohrabi, F. and W. Yu, "Hybrid analog and digital beamforming for OFDM-based large-scale MIMO systems," *IEEE International Workshop on Signal Processing Advances in Wireless Communications*, 1–6, 2016.
18. Balanis, C., *Antenna Theory*, Wiley, 1997.
19. Zhang, J., A. Wiesel, and M. Haardt, "Low rank approximation based hybrid precoding schemes for multi-carrier single-user massive MIMO systems," *IEEE International Conference on Acoustics, Speech and Signal Processing*, 3281–3285, 2016.
20. Musheng, W., "Perturbation theory for the eckart-young-mirsky theorem and the constrained total least squares problem," *Linear Algebra and Its Applications*, Vol. 280, No. 2, 267–287, 1998.